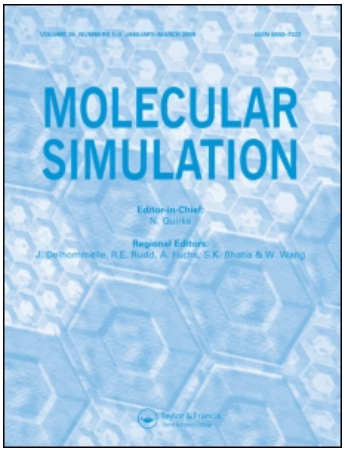

Molecular Simulation
Publication details, including instructions for authors and subscription information:
http://www.informaworld.com/smpp/title~content=t713644482

Reaction free energies in organic solvents: comparing different quantum mechanical methods

Ivan A. Konstantinov[a]; Linda J. Broadbelt[a]
[a] Department of Chemical and Biological Engineering, Northwestern University, Evanston, IL, USA

First published on: 22 January 2010

To cite this Article Konstantinov, Ivan A. and Broadbelt, Linda J.(2010) 'Reaction free energies in organic solvents: comparing different quantum mechanical methods', Molecular Simulation, 36: 15, 1197 — 1207, First published on: 22 January 2010 (iFirst)
To link to this Article: DOI: 10.1080/08927020903483288
URL: http://dx.doi.org/10.1080/08927020903483288

Molecular Simulation
Vol. 36, No. 15, December 2010, 1197–1207

Taylor & Francis
Taylor & Francis Group

Reaction free energies in organic solvents: comparing different quantum mechanical methods

Ivan A. Konstantinov and Linda J. Broadbelt*

Department of Chemical and Biological Engineering, Northwestern University, Evanston, IL 60208, USA

(*Received 31 August 2009; final version received 12 November 2009*)

A variety of quantum mechanical (QM) methods, basis sets and solute cavity descriptions using the conductor-like polarisable continuum model for the modelling of reaction free energies in solution have been evaluated and compared. In order to test the performance of each QM level of theory and cavity model, five common types of organic reactions in different solvents have been considered. The study shows that the hybrid metageneralised-gradient approximation M05-2X functional, in conjunction with the MG3S basis set and UA0 or universal force field cavities, produces results in the best overall agreement with experimental data. In addition, within the UA0 formalism, explicit cavities should be built on the hydrogen atoms that undergo transformation during chemical reaction.

Keywords: density functional theory; *ab initio*; conductor-like polarisable continuum model; reaction free energies; organic solvents

1. Introduction

The ability to accurately describe chemical reactions at the atomistic level can be essential to their design. The results of quantum mechanical (QM) calculations can suggest optimal modification of the functional groups of the reactants, guide the choice of solvents or improve existing catalysts in order to tune the efficiency of processes vital to many chemical and biological applications. Composite QM methods, such as G3B3 [1] and CBS-QB3 [2], allow the calculation of gas-phase heats of reaction for reactions involving relatively small molecules with an accuracy of 1–2 kcal/mol. Unfortunately, such precision in the condensed phase for a diverse spectrum of species and solvents is still elusive. This is in spite of the fact that numerous chemical reactions occur in solvents, where the formation of polar and ionic species renders such processes more thermodynamically and/or kinetically favourable than their gas-phase counterparts [3,4]. Hence, methodologies that produce accurate calculations of kinetic and thermodynamic properties for reactions in the presence of solvents are of utmost importance.

In the condensed phase, solvent–solvent and solvent–solute interactions increase the degree of complexity of the problem dramatically. Currently, there are several computational approaches that are commonly used that enable the modelling of reactions in the condensed phase at the QM level. Broadly, the methods fall into two classes: explicit and implicit solvation models.

Explicit solvation models are the most detailed and computationally intensive. They incorporate the solute and several solvation spheres of the solvent explicitly. Due to the large number of molecules and their interactions, this approach rapidly becomes very expensive, and its general application is limited to low levels of theory and only a few solvation spheres [5]. A more computationally economical technique is to separate the system into two parts: one treated at the QM level and another modelled using classical methods. While this hybrid quantum–molecular mechanics procedure is more practical, it is dependent on the development of accurate force fields and charge distribution schemes and their interface with the QM part of the system [5].

Implicit solvation models offer a fast and accurate alternative. Currently, the ones that are most frequently and successfully applied include the polarisable continuum model (PCM) [6–13], the conductor-like polarisable continuum model (C-PCM) [14], COSMO [15,16], SS(V)PE [17] and SM8 [18]. The details of the various solvation models and their formalism have been described elsewhere [6–19]. In addition to choosing which implicit solvation model is used, it is still necessary to select a QM level of theory and basis set, which can result in a staggering number of choices. Furthermore, different software packages do not include the same implicit solvation models, which may lead researchers to choose a method that is ill-suited to their particular problem.

Generally, the accuracy of implicit solvation models is increased if one or more explicit solvent molecules are included along with the solute [5,20]. This method is known as supramolecular or cluster-continuum. Nevertheless, the studies of Takano and Houk [21], Liptak et al. [22–24], da Silva et al. [25], Pliego and Riveros [26], Klamt et al. [27] and Kallies and Mitzner [28] have shown

*Corresponding author. Email: broadbelt@northwestern.edu

ISSN 0892-7022 print/ISSN 1029-0435 online

DOI: 10.1080/08927020903483288
http://www.informaworld.com

that pure dielectric models can achieve the accuracy of the cluster-continuum theory in an aqueous medium.

In this paper, we focus on the C-PCM as implemented in the Gaussian 03 program [29]. The C-PCM is a robust choice as an implicit solvation model that has been shown to have fewer convergence problems for medium to large size systems than alternative approaches in addition to providing very accurate results at a low computational cost [14,21].

While we focus exclusively on the C-PCM, there are still a number of choices that must be made for its implementation, and, thus, a review of the major features of the method is provided here. Within the C-PCM framework, the solvent is treated as a dielectric continuum described by its permittivity constant (ε). The solute, on the other hand, is placed in a cavity within the dielectric continuum. One of the major determinants of the accuracy of a solvation model is the construction of the solute cavity and the use of correct boundary conditions on its surface. In the C-PCM, the cavity is built with interlocking spheres centred on solute atoms or groups of atoms with specific van der Waals radii. The resulting surface is then smoothed by the addition of extra spheres not centred on individual atoms or groups. Once the surface is defined, it is divided into small triangular regions called tesserae that are characterised by their area, positions of the centres and the electrostatic vectors passing through the tesserae centres. Gaussian 03 provides the user with choices for the van der Waals radii as well as additional manipulation of the relevant cavity parameters. The schemes for specifying the van der Waals radii include the Bondi [30], Pauling [31], UA0, UAKS and UAHF [32] descriptions.

At the heart of the C-PCM is the calculation of the free energy in solution according to the formula

$$G_{\text{solution}} = G_{\text{electrostatic}} + G_{\text{cavitation}} + G_{\text{dispersion-repulsion}}, \tag{1}$$

where $G_{\text{electrostatic}}$ is the electrostatic contribution whose value is calculated using the self-consistent reaction field approach within the C-PCM formalism. Most cavity models that are compatible with the C-PCM use van der Waals radii which are optimised for aqueous media. In addition, a radii scaling factor ($f > 1$), which is solvent dependent and accounts for the fact that the first solvation sphere has different dielectric properties than the bulk, is introduced for the calculation of the electrostatic component of the free energy. Therefore, when applied to organic solvents, reoptimisation of the cavity description may be necessary. To this end, studies that prescribe different scale factors (f) for the calculation of solvation free energies in non-aqueous solvents are present in the literature [33–36]. However, these studies suggest that parameterisation of the solute cavity is strongly dependent on the solvation model, solvent, level of theory and basis set used. Moreover, a universal approach is currently not available.

The next free energy component in Equation (1), $G_{\text{cavitation}}$, is the free energy penalty associated with building the solute cavity whose value is determined by a modified Pierotti formula [8,37] to account for the non-spherical shape of the cavity. Finally, the $G_{\text{dispersion-repulsion}}$ term describes the van der Waals interactions between the solute and the surrounding solvent and is calculated according to the prescription of Floris and Tomasi [38] and Floris et al. [39].

One common approach to accurately calculate reaction free energies in solution is a thermodynamic cycle, such as the one shown in Figure 1 for a reaction A + B → C + D. This method allows for the calculation of the reaction free energy in the condensed phase, $\Delta G^0_{(\text{sol})}$, using Equation (2)

$$\Delta G^0_{(\text{sol})} = \Delta G^0_{(\text{gas})} + \Delta G^0_{\text{S}}(\text{C}) + \Delta G^0_{\text{S}}(\text{D}) - \Delta G^0_{\text{S}}(\text{A}) - \Delta G^0_{\text{S}}(\text{B}), \tag{2}$$

where $\Delta G^0_{\text{S}}(i)$ is the solvation free energy of component i. While correct solvation free energies are one important component of the thermodynamic cycle approach, it also necessitates accurate calculation of the energy in the gas phase, $\Delta G^0_{(\text{gas})}$. This is performed with much more expensive methodologies. Furthermore, the use of a thermodynamic cycle is not always possible. In certain cases, a species along the reaction coordinate may either be unstable in the gas phase or its geometry may be significantly different from that in solution. Hence, full optimisation in the condensed phase is demanded. Furthermore, most cavity optimisations use relatively low levels of theory to compute solvation free energies of the individual species. This is generally sufficient when a molecule goes from the gas phase to the condensed phase without undergoing any significant structural changes, such as bond breaking or bond forming. Within a thermodynamic cycle, the accuracy of these chemical transformations is captured through a high level of theory in the gas-phase calculation. If the thermodynamic cycle approach is not used, the condensed-phase calculations need to incorporate both the solvation of individual species and the effects of the solvent on the intra- or intermolecular change due to reaction accurately.

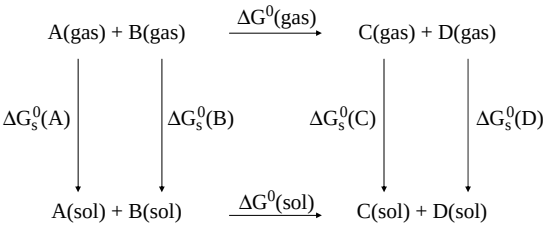

Figure 1. Thermodynamic cycle for the calculation of free energy of reaction in solution.

This study aims to benchmark the performance of a series of QM methods and basis sets that are frequently used with the C-PCM solvation model and the default solute cavity descriptions as implemented in Gaussian 03. Five different reactions were explored: tautomerisation of *N*,*N*-dimethylglycine, nucleophilic addition between acetone and methanol, dimerisation of nitrosobenzene, S_N2 reaction between N_3^- and *n*-BuBr, and S_N2 reaction between CN^- and $PhCH_2Cl$. For the first three reactions, free energies of reaction were computed and compared to experimental works. For the latter two reactions, free energies of activation were evaluated. Based on the performance of the different methods for all five reactions, a QM method, basis set and cavity description were recommended. While not adjusted here, further work could be carried out using the recommended method to adjust the cavity parameter to fine tune the results for a particular system of interest.

2. Computational details

The Gaussian 03 software package was employed for the calculations in this study. All geometries were optimised in the condensed phase using Becke's three-parameter hybrid exchange functional (B3) [40], the correlation functional of Lee, Yang and Parr (LYP) [41] and the 6-31+G(d,p) basis set [42–44]. This method is sufficient to ensure structural accuracy due to heteroatom polarisation, anionic effects and intramolecular hydrogen bond interactions at a reasonable computational cost. In order to explore the effects of the theoretical level on the calculated reaction free energies, single-point energy calculations at the B3LYP/6-311+G(d,p), B3LYP/MG3S, MP2/6-31++G(d,p), MP2/6-311+G(d,p), MP2/MG3S, MPWB1K/MG3S and M05-2X/MG3S levels of theory were performed, where MP2 is a post-Hartree–Fock (HF) method based on the Möller–Plesset theory [45], and MPWB1K and M05-2X are hybrid metageneralised-gradient approximations within density functional theory developed by Truhlar and co-workers [46,47]. The MG3S basis set is identical to the MG3 basis set [48], except it omits diffuse functions on hydrogen atoms. MG3, also known as the G3MP2Large basis set [49], is the modified G3Large basis set [50] and is effectively equal to the 6-311++G(3d2f,2df,2p) basis set for H–Si, but it is improved for P–Ar. For elements beyond the third row in the periodic table, for which MG3S is not available, the 6-311+G(2df,2p) basis set was used.

The geometry with the lowest electronic energy of all species and transition states (TSs) was found by a combination of conventional optimisation and one-dimensional potential energy dihedral scans. In the case of the TSs, the bond corresponding to the formation of the TS was kept frozen during all dihedral scans. All TSs were verified by the presence of a single imaginary frequency and its visualisation to ensure that the TS led to the reactants and products of interest. The temperature correction to the free energy was calculated using the frequencies from the full solvent optimisations at the B3LYP/6-31+G(d,p) level of theory with the harmonic oscillator approximation by means of standard formulae from statistical thermodynamics [51]. In addition, all frequencies were scaled by the prescription of Scott and Radom [52] for gas-phase calculations at the B3LYP/6-31G(d) level of theory because no methodology is available for condensed phases and the basis set used in this study. Finally, the free energy calculation includes all electrostatic and non-electrostatic components.

Gaussian 03 allows for the use of several predefined solute cavity descriptions as well as their modification. These are Bondi, Pauling, universal force field (UFF), UA0, UAKS and UAHF. The first three methods treat all hydrogen atoms explicitly, while the last three are variations of the united atom topological model (UATM) [32] and group the hydrogens with the nearest heavy atom. The UA0 cavity is constructed using the UATM applied on atomic radii of the UFF. UAKS and UAHF use UATM radii optimised for the PBE0/6-31G(d) and HF/6-31G(d) levels of theory, respectively [32]. In our study, the UAHF cavity description was applied only with MP2 single-point energy calculations on B3LYP-optimised geometries with UAKS. The default parameters, such as the electrostatic scaling factor (f), overlap index between interlocking spheres, the average tesserae area, etc., were employed for each cavity model. Finally, the dielectric constants (ε) used in this study were 4.9, 20.7, 32.63, 46.7 and 78.39 for chloroform, acetone, methanol, DMSO and water, respectively.

3. Results and discussion

Five organic reactions of different types under various reaction conditions were investigated. A scheme of the five specific reactions examined is presented in Figure 2. The first three reactions aim to examine the accuracy of the overall reaction free energy calculations, while the last two address the question of modelling free energies of activation. The results for each reaction are presented and discussed in turn below.

3.1 Tautomerisation of N,N-dimethylglycine

Amino acids are species vital to many chemical and biological processes. They can exist in two general neutral forms: uncharged and zwitterionic. The functional form of these species is dictated by their ability to be solvated in the media in which they are present. The molecular transformations that occur within the amino acids involve protonation and deprotonation of the carboxylic and amino moieties. Given that most amino acids are insoluble in

Reaction 1. Tautomerisation of *N*,*N*-dimethylglycine

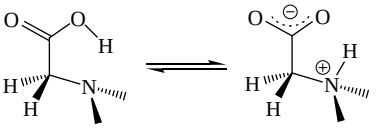

Reaction 2. Nucleophilic addition between acetone and methanol

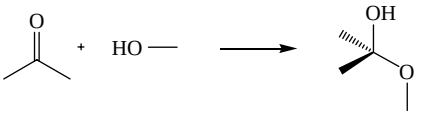

Reaction 3. Dimerisation of nitrosobenzene

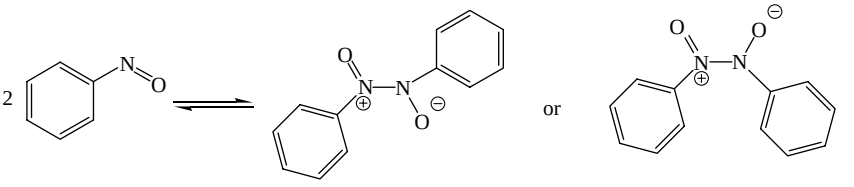

Reaction 4. Formation of S_N2-type transition state in the azide attack on *n*-BuBr

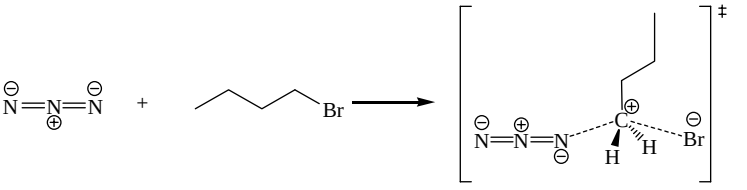

Reaction 5. Formation of S_N2-type transition state in the cyanide attack on $PhCH_2Cl$

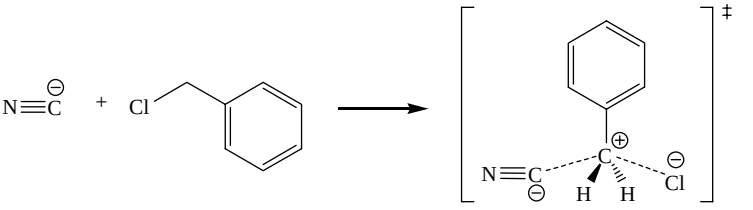

Figure 2. Schematics of the reactions examined in this study.

a large spectrum of organic solvents, accurate thermodynamic data are hard to obtain. However, alkylated amino acids are soluble in a variety of organic solvents, and experimental data for their free energy of reaction can be benchmarked to determine a methodology that may be extensible to a wide variety of systems. Thus, we chose the *N*,*N*-dimethylglycine system due to the available experimental data in acetone, DMSO, methanol and water. Furthermore, it is a relatively small system, and stabilisation of the zwitterionic form is not possible in the gas phase, rendering the thermodynamic cycle approach not applicable. Thus, the tautomerisation in the condensed phase is governed solely by the solvation of the zwitterion and provides a rigorous test of the ability of a computational methodology to predict reaction free energies in solution.

Figure 3 summarises the differences between the calculated and experimental reaction free energies in acetone and DMSO for a variety of computational methodologies. Both solvents are aprotic and poor hydrogen bond donors, but could act as acceptors, with DMSO acting as the better acceptor [53]. Experimental observations show that, at room temperature, *N*,*N*-dimethylglycine is present predominantly as a zwitterion (61% in acetone and 69% in DMSO), and the experimental free energies of reaction are -0.26 and -0.47 kcal/mol in acetone and DMSO, respectively [54]. Figure 3 shows that the use of Bondi and Pauling radii predicts reaction free energies that are more negative by 4.94–9.73 kcal/mol for both solvents. UFF radii perform significantly better. For most methods, the absolute error is less than 3 kcal/mol, with the best results achieved for MPWB1K/MG3S

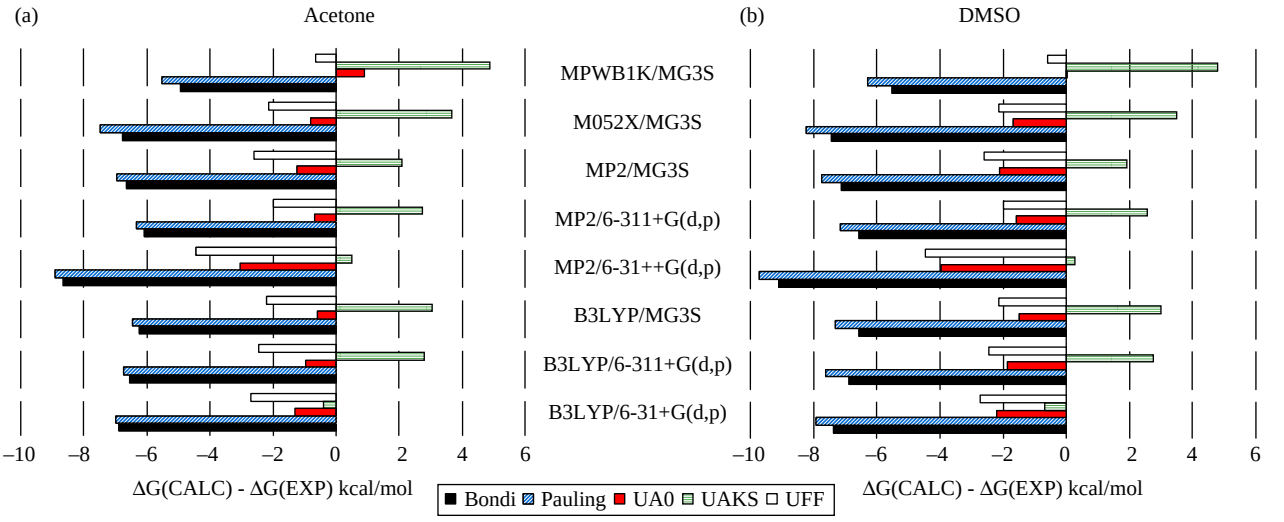

Figure 3. Tautomerisation of *N*,*N*-dimethylglycine at 298.15 K in (a) acetone and (b) DMSO. Experimental Gibbs free energies were taken from [54].

(absolute errors equal to 0.65 and 0.58 kcal/mol) and the worst for MP2/6-31++G(d,p) (absolute errors equal to 4.43 and 4.46 kcal/mol) for acetone and DMSO, respectively. However, UFF also consistently predicts free energies of reaction that are too negative, resulting in a higher zwitterionic population than is observed experimentally. UAKS/UAHF gives errors within 1 kcal/mol when B3LYP/6-31+G(d,p) and MP2/6-31++G(d,p) are used. This could be attributed to the fact that while both double- and triple-ξ basis sets accurately describe the molecular transformation, double-ξ basis sets capture the solvation of the species better in acetone and DMSO. Hence, while the addition of diffuse functions does not improve the quality of the results, expansion of the basis set to triple-ξ has a more pronounced effect. Finally, it is clear that UA0 performs very well (close to or less than an absolute error of 2 kcal/mol) for the majority of the computational methods used. The only exception is MP2/6-31++G(d,p) with errors greater than −4 kcal/mol for both acetone and DMSO. It is likely that the extra diffuse function on the hydrogen atoms, which overpredicts the bonding between the strongly negative carboxylic oxygen and the hydrogen in the amino group in the zwitterion, is responsible. As a result, the structure is overstabilised. This same method also produced the worst results when the UFF, Bondi and Pauling models were employed.

Comparison of the calculated and experimental free energies of reaction for conversion in methanol and water solvents is presented in Figure 4. These are two very polar solvents with the ability to be both hydrogen bond acceptors and donors. Nevertheless, the trends are very similar to those discussed above. Bondi and Pauling again markedly overpredict the preference for the zwitterion. UFF also favours the zwitterionic form too heavily, but the errors are lower and close to those observed for acetone and DMSO. An interesting difference compared to the acetone and DMSO results is observed when UAKS/UAHF cavities are used. The use of double-ξ basis sets gives poorer results than triple-ξ basis sets. This is unexpected because these methodologies are optimised for an aqueous medium with doubly split valence functions. However, these cavity models are adjusted against a limited set of experimental data which does not include zwitterionic species. Hence, for protic polar solvents, valence expansion of the basis set could be important in order to capture the tautomeric process. Employing UA0 again produces very small errors; although the error with MPWB1K is higher than it was for DMSO and acetone, it is still within 2 kcal/mol.

3.2 Nucleophilic addition between acetone and methanol

Association reactions are difficult to model at the QM level, and accurate results are particularly sensitive to the theoretical methods used. Generally, large basis sets or high levels of theory are employed. In order to test the performance of the five solute cavity descriptions, we chose the nucleophilic addition reaction between acetone and methanol in methanol, which results in the formation of a tetrahedral product. The formation of such structures is the cornerstone of many proposed stepwise reaction mechanisms in which they appear as reaction intermediates [3,4]. However, the creation of tetrahedral species is very hard to measure experimentally because they often lie high on the reaction free energy surface and their lifetime is extremely short [4,55]. Therefore, the accurate prediction

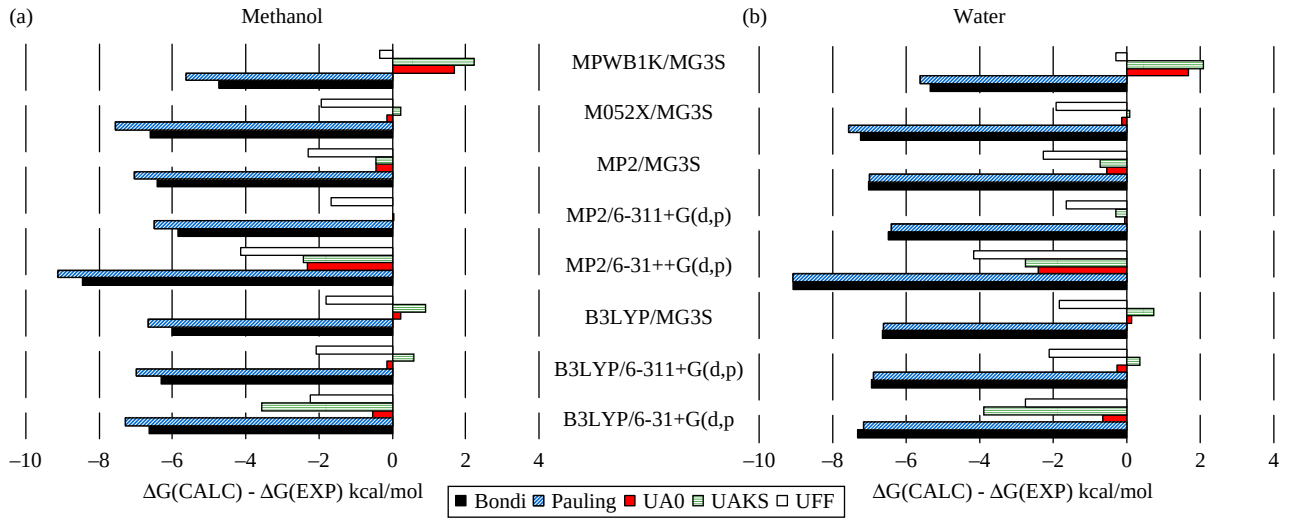

Figure 4. Tautomerisation of *N*,*N*-dimethylglycine at 298.15 K in (a) methanol and (b) water. Experimental Gibbs free energies were taken from [54].

of such intermediates is essential for the atomistic rationalisation of many chemical processes.

Figure 5 shows the results for the reaction free energies. Unfortunately, optimisation of acetone in methanol using a Pauling cavity was not achieved, and thus these results are not included. The results indicate that UA0 consistently produces the smallest error at every level of theory compared to Bondi, UAKS/UAHF and UFF. The smallest errors are obtained at the MP2/MG3S and M05-2X/MG3S levels of theory. The results are consistent with the fact that experimental data are typically best captured using either post-HF methods, such as MP2, or methods including parameterisation and increased HF exchange such as MPWB1K and M05-2X coupled with the large MG3S basis set.

3.3 Dimerisation of nitrosobenzene

Dimerisation of nitrosobenzene is another example of an association reaction. However, this process results in the formation of two distinct isomers, *cis* and *trans*, as defined by the position of the oxygen atoms and the phenyl rings with respect to the nitrogen–nitrogen double bond. As a consequence, accurate modelling at the QM level should reflect both the relative stability of the two isomers as well as the reaction free energy of dimerisation. The computational results for the different combinations of cavity descriptions and levels of theory are illustrated in Figure 6. Experimentally, the *cis*-isomer is observed to be thermodynamically preferred [56]. The B3LYP functional performs poorly; it not only severely underestimates the

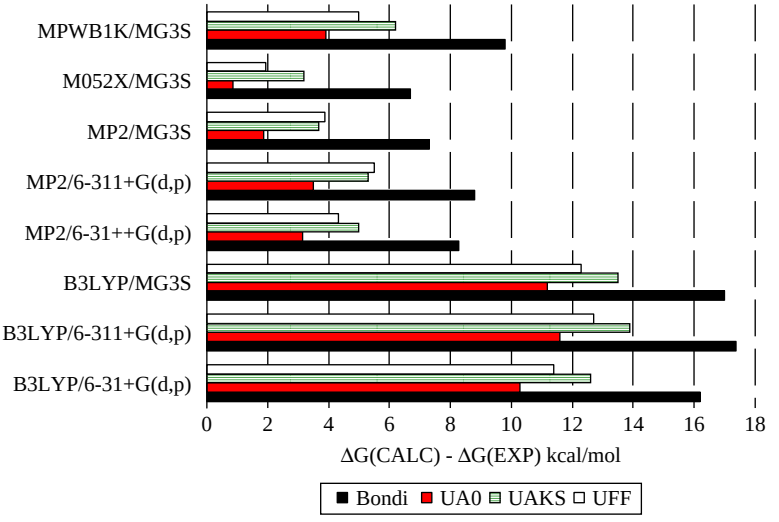

Figure 5. Nucleophilic addition between acetone and methanol in methanol at 298.15 K. Standard state 1 M. A correction factor of $-RT\ln 2$ was included to account for the enantiomeric tetrahedral product. Experimental Gibbs free energies were taken from [55].

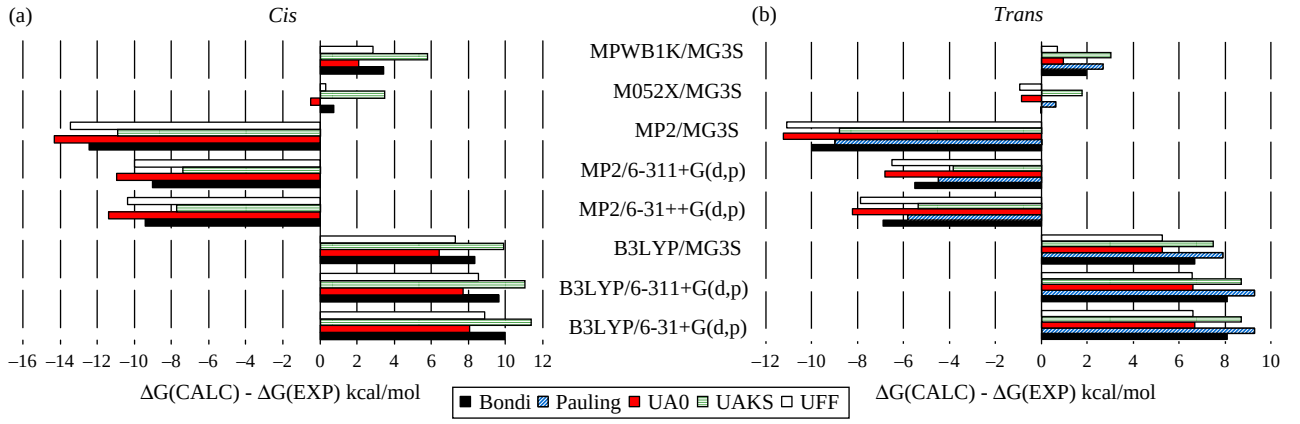

Figure 6. Dimerisation of nitrosobenzene in chloroform at 298.15 K. Standard state 1 M. Experimental Gibbs free energies were taken from [56].

extent of dimerisation, but it also predicts that the *trans*-isomer is more stable regardless of the cavity model used. MP2 is similarly poor; it also overestimates the extent to which the dimer is formed, although it captures the relative stability of the two isomers correctly. The absolute error varies between 5.27 and 11.4 kcal/mol for B3LYP and 3.83 and 14.3 kcal/mol for MP2. Even though M05-2X gives relatively accurate reaction free energy values with UFF and Bondi, the relative isomer stability is inverted. Optimisation of the *cis*-dimer with Pauling was not achieved; however, the results for the *trans* species with the Pauling cavity and the M05-2X/MG3S level of theory were very close to the experimental data. The MPWB1K/MG3S results were an improvement when compared to the MP2 and B3LYP results in terms of reaction free energy, but as seen with B3LYP, the relative stability of the two dimers was incorrectly captured. Finally, the best overall results for the dimerisation of nitrosobenzene were obtained with M05-2X/MG3S and UA0.

3.4 S_N2 reaction between N_3^- and n-BuBr

Free energies of activation are of particular interest to theoreticians as well as experimentalists because they allow for the calculation of reaction rate coefficients via TS theory and thus allow questions about both the thermodynamic and kinetic feasibility of chemical and biological processes to be answered. S_N2-type reactions are very common in organic chemistry and involve TS in which simultaneous bond breaking and bond forming occur when a nucleophilic molecule attacks an electrophile. Here, we calculated the free energy of activation when N_3^- displaces the bromide atom in *n*-BuBr in both DMSO and methanol. Experimentally, the reaction rate is over 600 times faster in DMSO than in methanol [57]. The results of the calculations for the different combinations of cavity descriptions and levels of theory are shown in Figure 7. Our calculations show that, for DMSO, all combinations of methods and solute cavity descriptions overpredict the free energy barrier to various degrees. The best outcome is achieved using the M05-2X functional with UFF and UA0, where the error is less than 0.5 kcal/mol. N_3^- in DMSO could not be optimised at B3LYP/6-31+g(d,p) with UAKS, which underscores the idea that full optimisation in the condensed phase can be a challenging task. In methanol, it is difficult to distinguish consistent trends. Bondi and Pauling radii performed rather well for a number of different methods. The free energy of activation is captured with an absolute error smaller than 1 kcal/mol when B3LYP/6-311+G(d,p), B3LYP/6-311+G(2df,2p) or M05-2X/6-311+G(2df,2p) is used. UA0 with M05-2X/6-311+G(2df,2p) shows a large absolute error, which is in stark contrast to how well this method performed for the other reactions in this study. Interestingly, M05-2X/6-311+G(2df,2p) with UFF gives deviation from experimental results smaller than 0.5 kcal/mol, as observed for DMSO.

3.5 S_N2 reaction between CN^- and $PhCH_2Cl$

In order to further test the performance of the different methods in predicting free energies of activation, the formation of the TS between CN^- and $PhCH_2Cl$ in methanol was studied. The results are summarised in Figure 8. Here, the best results were obtained for M05-2X/MG3S with UFF or UA0. It is worth noting that, while the MP2 method overpredicts the reaction barrier, the B3LYP functional underpredicts it regardless of the basis set and cavity employed. Generally, the results of the free energies of activation in Figure 8 confirm that even though cavity descriptions such as UA0, UAKS and UAHF are optimised for molecules at their minimum energy states, they can be translated to TS as well.

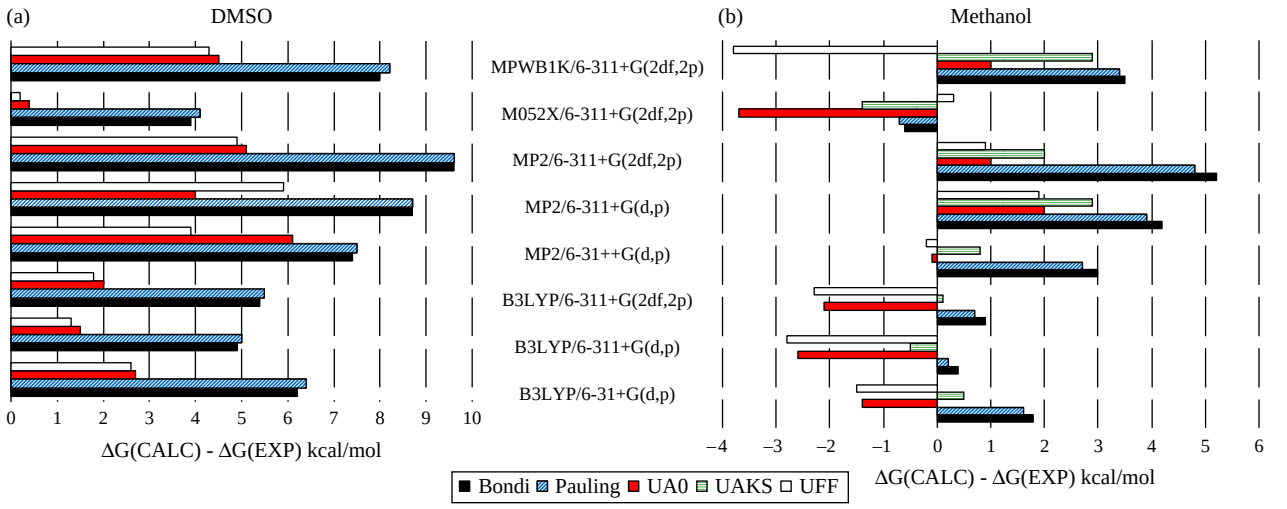

Figure 7. S_N2 reaction between N_3^- and *n*-BuBr at 333.15 K in (a) DMSO and (b) methanol. Standard state 1 M. Experimental Gibbs free energies were taken from [57].

3.6 Discontinuities in the construction of reaction coordinates

The results so far indicate that the UA0 and UFF cavity descriptions, in conjunction with the M05-2X/MG3S level of theory, produce the smallest errors from the experimental reaction free energies under a variety of reaction conditions. However, using UA0, or other UATM cavities, for modelling reaction coordinates involving hydrogen transfer has been criticised because such solute cavity descriptions create discontinuities between the reactants, product, intermediates and the transition states that connect them. The problem arises due to the fact that hydrogen atoms are part of the envelope of the nearest heavy atom. For this reason alone, many researchers rely on solute cavities built with explicit spheres on the hydrogen atoms. An alternative approach suggested by Barone and Cossi during the development of the UATM formalism was to build explicit cavities around the acidic hydrogens that undergo movement during the reaction [32]. To test this methodology, we compared the results for UA0 with and without explicit cavities around the hydrogen atoms that transfer at the M05-2X/MG3S

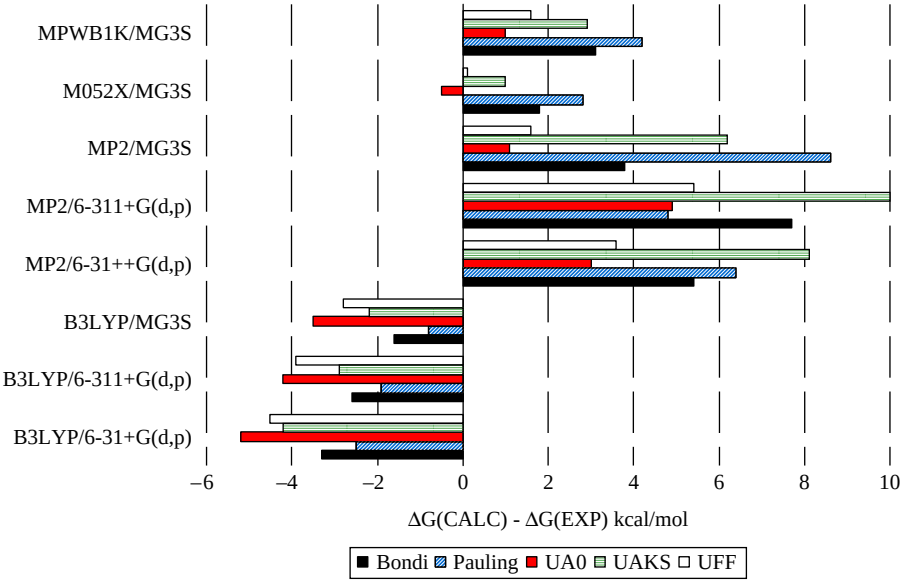

Figure 8. S_N2 reaction between CN^- and $PhCH_2Cl$ in methanol at 333.15 K. Standard state 1 M. Experimental Gibbs free energies were taken from [57].

Table 1. Comparison of the UA0 and UA0(H) cavity descriptions[a,b].

Reaction	Solvent	Cavity model	
		UA0	UA0(H)[c]
1	Acetone	−0.80	−0.18
	DMSO	−1.69	−0.47
	Methanol	−0.15	0.10
	Water	−0.13	0.30
2	Methanol	0.87	0.36

[a] All calculations were performed using M05-2X/MG3S//B3LYP/6-31+G(d,p). [b] The values (kcal/mol) represent deviation from experimental reaction Gibbs free energies and were calculated as $\Delta G_{(calc)} - \Delta G_{(exp)}$. [c] UA0(H) symbolises the UA0 cavities with explicit spheres on hydrogen atoms that undergo chemical transformations and is applicable only to reactions 1 and 2.

theoretical level. The results are summarised in Table 1. Direct comparison of the two approaches reveals that building an explicit cavity around the acidic hydrogen results in a minor change in the reaction free energies. The majority of the errors remain within 0.5 kcal/mol. The highest deviation is present for DMSO where the discrepancy rises to 1.22 kcal/mol, with the explicit hydrogen cavity providing the lower error.

4. Conclusion

In this study, the performance of the C-PCM, as implemented in the Gaussian 03 software package, in calculating free energies in solution for a set of common organic reactions, solvents and QM levels of theory was assessed. We recommend the use of the M05-2X/MG3S functional and basis set along with the UA0 solute cavity description with explicit spheres on the hydrogens that undergo chemical transformations for the construction of free energy reaction coordinates. This methodology showed very good results for the relative stability of reactants and products, as well as free energies of activation. Another method that produced relatively accurate results was M05-2X/MG3S with UFF radii. The overall performance of the M05-2X/MG3S level of theory with the UA0 and UFF cavities for the reactions investigated in this study is summarised in Table 2.

Table 2. Overall performance of the UFF and UA0/UA0(H) cavity models[a,b].

Reaction	Solvent	Cavity model			
		UFF		UA0/UA0(H)[c]	
1	Acetone	−2.13		−0.18	
	DMSO	−2.15		−0.47	
	Methanol	−1.95		0.10	
	Water	−1.91		0.30	
2	Methanol	1.94		0.36	
		cis	*trans*	*cis*	*trans*
3	Chloroform	0.32	−0.95	−0.53	−0.88
4[d]	DMSO	0.20		0.40	
	Methanol	0.30		−3.70	
5	Methanol	0.10		−0.50	

[a] All calculations were performed using M05-2X/MG3S//B3LYP/6-31+G(d,p) unless additionally noted. [b] The values (kcal/mol) represent deviation from experimental reaction Gibbs free energies and were calculated as $\Delta G_{(calc)} - \Delta G_{(exp)}$. [c] UA0(H) symbolises the UA0 cavities with explicit spheres on hydrogen atoms that undergo chemical transformations and is applicable only to reactions 1 and 2. [d] Calculations were performed using M05-2X/6-311+G(2df,2p)//B3LYP/6-31+G(d,p).

Acknowledgements

Funding through the Institute for Catalysis in Energy Processes (ICEP) at Northwestern University which is sponsored by DOE is acknowledged. Computational resources used for this study were available through NERSC.

References

[1] A.G. Baboul, L.A. Curtiss, and P.C. Redfern, *Gaussian-3 theory using density functional geometries and zero-point energies*, J. Chem. Phys. 110 (1999), pp. 7650–7657.
[2] J.A. Montgomery, M.J. Frisch, J.W. Ochterski, and G.A. Petersson, *A complete basis set model chemistry. VI. Use of density functional geometries and frequencies*, J. Chem. Phys. 110 (1999), pp. 2822–2827.
[3] F.A. Carey, *Organic Chemistry*, 5th ed., McGraw-Hill, New York, NY, 2002.
[4] J. Clayden, N. Greeves, S. Warren, and P. Wothers, *Organic Chemistry*, Oxford University Press, Oxford, 2000.
[5] C.J. Cramer, *Essentials of Computational Chemistry: Theories and Models*, 2nd ed., Wiley, Chichester, 2004.
[6] S. Miertus, E. Scrocco, and J. Tomasi, *Electrostatic interaction of a solute with a continuum. A dielectric utilization of* ab initio *molecular potentials for the prevision of solvent effects*, Chem. Phys. 55 (1981), pp. 117–129.
[7] S. Miertus and J. Tomasi, *Approximate evaluations of the electrostatic free energy and internal energy changes in solution processes*, Chem. Phys. 65 (1982), pp. 239–245.
[8] M. Cossi, V. Barone, R. Cammi, and J. Tomasi, Ab initio *study of solvated molecules: A new implementation of the polarizable continuum model*, Chem. Phys. Lett. 255 (1996), pp. 327–335.
[9] E. Cances, B. Mennucci, and J. Tomasi, *A new integral equation formalism for the polarizable continuum model: Theoretical background and applications to isotropic and anisotropic dielectrics*, J. Chem. Phys. 107 (1997), pp. 3032–3041.
[10] B. Mennucci and J. Tomasi, *Continuum solvation models: A new approach to the problem of solute's charge and cavity boundaries*, J. Chem. Phys. 106 (1997), pp. 5151–5158.
[11] B. Mennucci, E. Cances, and J. Tomasi, *Evaluation of solvent effects in isotropic and anisotropic dielectrics and in ionic solutions with a unified integral equation method: Theoretical bases, computational implementations, and numerical applications*, J. Phys. Chem. B 101 (1997), pp. 10506–10517.
[12] M. Cossi, N. Rega, G. Scalmani, and V. Barone, *Polarizable dielectric model of solvation with inclusion of charge penetration effects*, J. Chem. Phys. 114 (2001), pp. 5691–5701.
[13] M. Cossi, G. Scalmani, N. Rega, and V. Barone, *New developments in the polarizable continuum model for quantum mechanical and classical calculations on molecules in solution*, J. Chem. Phys. 117 (2002), pp. 43–54.
[14] M. Cossi, N. Rega, G. Scalmani, and V. Barone, *Energies, structures, and electronic properties of molecules in solution with the C-PCM solvation model*, J. Comput. Chem. 24 (2002), pp. 669–681.

[15] V. Barone and M. Cossi, *Quantum calculation of molecular energies and energy gradients in solution by a conductor solvent model*, J. Phys. Chem. A 102 (1998), pp. 1995–2001.

[16] A. Klamt, *Conductor-like screening model for real solvents: A new approach to the quantitative calculation of solvation phenomena*, J. Phys. Chem. 99 (1995), pp. 2224–2235.

[17] D.M. Chipman, *Reaction field treatment of charge penetration*, J. Chem. Phys. 112 (2000), pp. 5558–5565.

[18] A.V. Marenich, R.M. Olson, C.P. Kelly, C.J. Cramer, and D.G. Truhlar, *Self-consistent reaction field model for aqueous and nonaqueous solutions based on accurate polarized partial charges*, J. Chem. Theor. Comput. 3 (2007), pp. 2011–2033.

[19] J. Tomasi, B. Mennucci, and R. Cammi, *Quantum mechanical continuum solvation models*, Chem. Rev. 105 (2005), pp. 2999–3093.

[20] F. Ding, J.M. Smith, and H. Wang, *First-principles calculation of pK_a values for organic acids in nonaqueous solution*, J. Org. Chem. 74 (2009), pp. 2679–2691.

[21] Y. Takano and K.N. Houk, *Benchmarking the conductor-like polarizable continuum model (CPCM) for aqueous solvation free energies of neutral and ionic organic molecules*, J. Chem. Theor. Comput. 1 (2005), pp. 70–77.

[22] A.M. Toth, M.D. Liptak, D.L. Phillips, and G. Shields, *Accurate relative pK_a calculations for carboxylic acids using complete basis set and Gaussian*-n *models combined with continuum solvation methods*, J. Chem. Phys. 114 (2001), pp. 4595–4606.

[23] M.D. Liptak and G. Shields, *Accurate pK_a calculations for carboxylic acids using complete basis set and Gaussian*-n *models combined with CPCM continuum solvation methods*, J. Am. Chem. Soc. 123 (2001), pp. 7314–7319.

[24] M.D. Liptak, K.C. Gross, P.G. Seybold, S. Feldgus, and G. Shields, *Absolute pK_a determinations for substituted phenols*, J. Am. Chem. Soc. 124 (2002), pp. 6421–6427.

[25] G. da Silva, E.M. Kennedy, and B.Z. Dlugogorski, Ab initio *procedures for aqueous-phase pK_a calculations: The acidity of nitrous acid*, J. Phys. Chem. A 110 (2006), pp. 11371–11376.

[26] J.R. Pliego, Jr and J.M. Riveros, *Free energy profile of the reaction between the hydroxide ion and ethyl acetate in aqueous and dimethyl sulfoxide solutions: A theoretical analysis of the changes induced by the solvent on the different reaction pathways*, J. Phys. Chem. A 108 (2004), pp. 2520–2526.

[27] A. Klamt, F. Eckert, and M. Diedenhofen, *First principles calculations of aqueous pK_a values for organic and inorganic acids using COSMO-RS reveal an inconsistency in the slope of the pK_a scale*, J. Phys. Chem. A 107 (2003), pp. 9380–9386.

[28] B. Kallies and R. Mitzner, *pK_a values of amines in water from quantum mechanical calculations using a polarized dielectric continuum representation of the solvent*, J. Phys. Chem. B 101 (1997), pp. 2959–2967.

[29] M.J. Frisch, G.W. Trucks, H.B. Schlegel, G.E. Scuseria, M.A. Robb, J.R. Cheeseman, J.J.A. Montgomery, T. Vreven, K.N. Kudin, J.C. Burant, J.M. Millam, S.S. Iyengar, J. Tomasi, V. Barone, B. Mennucci, M. Cossi, G. Scalmani, N. Rega, G.A. Petersson, H. Nakatsuji, M. Hada, M. Ehara, K. Toyota, R. Fukuda, J. Hasegawa, M. Ishida, T. Nakajima, Y. Honda, O. Kitao, H. Nakai, M. Klene, X. Li, J.E. Knox, H.P. Hratchian, J.B. Cross, V. Bakken, C. Adamo, J. Jaramillo, R. Gomperts, R.E. Stratmann, O. Yazyev, A.J. Austin, R. Cammi, C. Pomelli, J.W. Ochterski, P.Y. Ayala, K. Morokuma, G.A. Voth, P. Salvador, J.J. Dannenberg, V.G. Zakrzewski, S. Dapprich, A.D. Daniels, M.C. Strain, O. Farkas, D.K. Malick, A.D. Rabuck, K. Raghavachari, J.B. Foresman, J.V. Ortiz, Q. Cui, A.G. Baboul, S. Clifford, J. Cioslowski, B.B. Stefanov, G. Liu, A. Liashenko, P. Piskorz, I. Komaromi, R.L. Martin, D.J. Fox, T. Keith, M.A. Al-Laham, C.Y. Peng, A. Nanayakkara, M. Challacombe, P.M.W. Gill, B. Johnson, W. Chen, M.W. Wong, C. Gonzalez, and J.A. Pople, *Gaussian 03*, Gaussian, Inc, Wallingford, CT, 2003.

[30] A. Bondi, *van der Waals volumes and radii*, J. Chem. Phys. 68 (1964), pp. 441–451.

[31] R.C. Weast (ed.), *Handbook of Chemistry and Physics*, Chemical Rubber, Cleveland, OH, 1981.

[32] V. Barone, M. Cossi, and J. Tomasi, *A new definition of cavities for the computation of solvation free energies by the polarizable continuum model*, J. Chem. Phys. 107 (1997), pp. 3210–3221.

[33] J.R. Pliego, Jr and J.M. Riveros, *Parametrization of the PCM model for calculating solvation free energy of anions in dimethyl sulfoxide solutions*, Chem. Phys. Lett. 355 (2002), pp. 543–546.

[34] Y. Fu, L. Liu, R.-Q. Li, R. Liu, and Q.-X. Guo, *First-principles predictions of absolute pK_a's of organic acids in dimethyl sulfoxide solution*, J. Am. Chem. Soc. 126 (2004), pp. 814–822.

[35] Y. Fu, L. Liu, Y.-M. Wang, J.-N. Li, T.-Q. Yu, and Q.-X. Guo, *Quantum-chemical predictions of redox potentials of organic anions in dimethyl sulfoxide and reevaluation of bond dissociation enthalpies measured by the electrochemical methods*, J. Phys. Chem. A 110 (2006), pp. 5874–5886.

[36] J.-N. Li, L. Liu, Y. Fu, and Q.-X. Guo, *What are the pK_a values of organophosphorus compounds?* Tetrahedron 62 (2006), pp. 4453–4462.

[37] R. Pierotti, *A scaled particle theory of aqueous and nonaqueous solutions*, Chem. Rev. 76 (1976), pp. 717–726.

[38] F.M. Floris and J. Tomasi, *Evaluation of the dispersion contributions to the solvation energy. A simple computational model in the continuum approximation*, J. Comput. Chem. 10 (1989), pp. 616–627.

[39] F.M. Floris, J. Tomasi, and J.L. Pascual Ahuir, *Dispersion and repulsion contributions to the solvation energy: Refinements to a simple computational model in the continuum approximation*, J. Comput. Chem. 12 (1991), pp. 784–791.

[40] A.D. Becke, *Density-functional thermochemistry. III. The role of exact exchange*, J. Chem. Phys. 98 (1993), pp. 5648–5652.

[41] C. Lee, W. Yang, and R. Parr, *Development of the Colle–Salvetti correlation-energy formula into a functional of the electron density*, Phys. Rev. B 37 (1988), pp. 785–789.

[42] W.J. Hehre, R. Ditchfield, and J.A. Pople, *Self-consistent molecular orbital methods. XII. Further extensions of Gaussian-type basis sets for use in molecular orbital studies of organic molecules*, J. Chem. Phys. 56 (1972), pp. 2257–2261.

[43] P.C. Hariharan and J.A. Pople, *The influence of polarization functions on molecular orbital hydrogenation energies*, Theor. Chim. Acta 28 (1973), pp. 213–222.

[44] M.J. Frisch and J.A. Pople, *Self-consistent molecular orbital methods 25. Supplementary functions for Gaussian basis sets*, J. Chem. Phys. 80 (1984), pp. 3265–3269.

[45] C. Möller and M.S. Plesset, *Note on an approximation treatment for many-electron systems*, Phys. Rev. 46 (1934), pp. 618–622.

[46] Y. Zhao and D.G. Truhlar, *Hybrid meta density functional theory methods for thermochemistry, thermochemical kinetics, and noncovalent interactions: The MPW1B95 and MPWB1K models and comparative assessment for hydrogen bonding and van der Waals interactions*, J. Phys. Chem. A 108 (2004), pp. 6908–6918.

[47] Y. Zhao, N.E. Schultz, and D.G. Truhlar, *Design of density functionals by combining the method of constraint satisfaction with parametrization for thermochemistry, thermochemical kinetics, and noncovalent interactions*, J. Chem. Theor. Comput. 2 (2006), pp. 364–382.

[48] P.L. Fast, M.L. Sanchez, and D.G. Truhlar, *Multi-coefficient Gaussian-3 method for calculating potential energy surfaces*, Chem. Phys. Lett. 306 (1999), pp. 407–410.

[49] L.A. Curtiss, P.C. Redfern, K. Raghavachari, V. Rassolov, and J.A. Pople, *Gaussian-3 theory using Möller–Plesset order*, J. Chem. Phys. 110 (1999), pp. 4703–4709.

[50] L.A. Curtiss, K. Raghavachari, P.C. Redfern, V. Rassolov, and J.A. Pople, *Gaussian-3 (G3) theory for molecules containing first and second-row atoms*, J. Chem. Phys. 109 (1998), pp. 7764–7776.

[51] D.A. McQuarrie, *Statistical Mechanics*, University Science Books, Sausalito, CA, 2000.

[52] A. Scott and L. Radom, *Harmonic vibrational frequencies: An evaluation of Hartree–Fock. Möller–Plesset, quadratic configurational interactions, density functional theory, and semiempirical scale factors*, J. Phys. Chem. 100 (1996), pp. 16502–16513.

[53] E.V. Anslyn and D.A. Dougherty, *Modern Physical Organic Chemistry*, University Science Books, Sausalito, CA, 2006.

[54] A.D. Headley, R.E. Corona, and E.T. Cheung, *Effects of solvents on the tautomerization of* N,N-*dimethylglycine*, J. Phys. Org. Chem. 10 (1997), pp. 898–900.

[55] J.P. Guthrie, *Hydration of carboxylic acids and esters. Evaluation of the free energy change for addition of water to acetic and formic acids and their methyl esters*, J. Am. Chem. Soc. 95 (1973), pp. 6999–7003.

[56] K.G. Orrell, V. Sik, and D. Stephenson, *Study of the monomer–dimer equilibrium of nitrosobenzene using multinuclear one- and two-dimensional NMR techniques*, Mag. Res. Chem. 25 (1987), pp. 1007–1011.

[57] N. Furukawa, F.R. Takahashi, T. Yoshimura, and S. Oae, *A study of the solvent effect of dimethyl sulfoxamine on the rates of* S_N2 *reactions*, Chem. Lett. (1977), pp. 1359–1360.